Study of Poincare Maps, Cobweb Diagrams and the Dynamics of Chaotic Systems defined by the Lorenz and Rössler Equations

Emil S. Spasov

Department of Physics, Norwegian University of Science and Technology, 7491 Trondheim.

Abstract

This report explores intricate dynamics of nonlinear systems and studies the complex behaviors of the Lorenz and Rössler systems. We study the stability of two dimensional systems using Poincaré maps and cobweb diagrams. Through numerical analysis we show that the Lorenz and Rössler systems do not have limit cycles. We then compute the Lyapunov exponents, revealing the sensitive dependence on initial conditions which is characteristic of these chaotic systems. What we find is a subtle interplay between determinism and unpredictability. This shows that even chaos carries some useful information and provides a deeper understanding of the mechanisms that govern the behaviour of nonlinear systems.

1. Introduction

This report explores nonlinear dynamics, that introduce us to the behaviors and patterns within complex systems. We start with foundational concepts like Poincaré maps and cobweb constructions that help us understand how systems can stabilize over time. Then, we dive into the unpredictable nature of chaotic systems through the study of the Lorenz and Rössler equations.

Different numerical and computational methods are employed in order to estimate the Lyapunov exponents of the Lorenz and Rössler systems and explore the intriguing balance between order and chaos. By applying these techniques, we gain insights into the behavior of complex systems, offering a window into their long-term dynamics and the conditions under which they exhibit stability or descend into chaos.

2. Theory and Methods

For the numerical implementation of this assignment we are using *Julia v1.10.0* in the *Pluto.jl* environment, making extensive use of the *DifferentialEquations.jl*, *GLMakie.jl*, *LinearAlgebra.jl*, *Plots.jl* and a few others. In this study we will encounter many differential equations we have to integrate numerically. We will do that using the built in functions in DifferentialEquations.jl and applying the Tsitouras 5(4) Runge-Kutta method (often refered to as Tsit5(4)) due to it's high efficiency and precision [3].

2.1. Poincaré maps and Cobweb diagrams

Poincaré maps, also known as *return maps*, are useful for studying swirling flows in phase space, such as the flow near a periodic orbit or chaotic systems.

Consider an n dimensional system given by $\dot{\mathbf{x}} = \mathbf{f}(\mathbf{x})$. Let S be an $n-1$ dimensional surface, known as the *Poincaré section*. S is required to be transverse to the flow. Poincaré map P is a mapping from S to itself, obtained by following trajectories from one intersection with S to the next [1]. If $\mathbf{x_k} \in S$ denotes the $k-$th intersection, then the Poincaré map is defined by $\mathbf{x_{k+1}} = P(\mathbf{x_k})$.

A fixed point $\mathbf{x}^*$ on the Poincaré map then denotes a closed orbit as a trajectory starting at $\mathbf{x}^*$ returns to $\mathbf{x}^*$.

Cobweb diagrams allow us to effectively simulate iterations of the map and can be used to determine the qualitative nature of the dynamics. To obtain the Cobweb diagram we can sketch orbits of a one-dimensional map, such as $P(r)$, as follows. We first draw the 45° identity line, $y = r$. Given an initial value r_0, we start at the point (r_0, r_0), then draw a vertical line segment to the graph of $P(r)$, then continue with a horizontal line segment back to the 45° line. These two line segments take us to the point $(P(r), P(r))$ [1]. Continue this process for as many steps as you like. The points where the map $P(r)$ crosses the identity line are fixed points. If the system has a stable limit-cycle at some point, the cobweb converges to that point. [2].

In this report we will study two different systems given in polar coordinates as follows:

$$\begin{aligned} \dot{r} &= r(1 - r^2) \\ \dot{\theta} &= 4\pi \end{aligned} \tag{2.1.1}$$

and

$$\begin{aligned} \dot{r} &= A(r - \pi)e^{-\omega t} \\ \dot{\theta} &= \pi. \end{aligned} \tag{2.1.2}$$

Where A and ω are parameters. [2] In order to find the Poincaré map $P(r)$ we integrate numerically equations (2.1.1) and (2.1.2) and save the points $r(t)$, when $\theta(t) = \text{mod } 2\pi$. The method used is Tsit5 without the adaptive stepsize. This is because we require a certain number of iterations.

The Poincaré map of equation (2.1.1) can be obtained analytically [1] and has the following expression:

$$P_a(r) = \left[1 + e^{-1}(r^{-2} - 1)\right]^{-\frac{1}{2}} \tag{2.1.3}$$

Comparing the analytical expression given by eq. (2.1.3) with the numerical result $P_n(r)$ can give us the numerical error ϵ_r,

$$\epsilon_r = \frac{|P_a(r) - P_n(r)|}{|P_n(r)|} \cdot 100\% \tag{2.1.4}$$

2.2. Lorenz and Rössler System

We begin our study of chaos with the *Lorenz equations* that are among the most recognized examples of a system that can exhibit chaotic behavior. The system is given by:

$$\begin{aligned} \dot{x} &= \sigma(y - x), \\ \dot{y} &= x(\rho - z) - y, \\ \dot{z} &= xy - \beta z. \end{aligned} \tag{2.2.1}$$

where σ, ρ, $\beta > 0$ are free parameters. For this project we will consider $\sigma = 10$, $\rho = 28$, $\beta = \frac{8}{3}$.

Next we consider the *Rössler system* given by the equations:

$$\begin{aligned} \dot{x} &= -y - z, \\ \dot{y} &= x + ay, \\ \dot{z} &= b + z(x - c). \end{aligned} \tag{2.2.2}$$

where $a = 0.2$, $b = 0.2$, $c = 5.7$ are parameters.

Both systems have a *strange attractor* and experience chaos for the given values of the parameters. A strange attractor is an attractor which is sensitive to initial conditions [2]. We call a closed set A an attractor if:

1. Any trajectory that starts in A, stays in A at all times.
2. If sufficiently close, any trajectory will eventually end up in A.
3. There is no proper subset of A that satisfies 1 and 2.

Two trajectories starting close to each other should diverge quickly away from one another on the strange attractor. In general, the separation distance $||\delta(t)||$ between the two endpoints $\mathbf{x_1}$ and $\mathbf{x_0}$ on two different trajectories increases exponentially:

$$||\delta(t)|| = ||\mathbf{x_1} - \mathbf{x_0}|| \sim \delta_0 e^{\lambda t} \tag{2.2.3}$$

where the constant λ often is referred to as the *Liapunov exponent*.

To find the first Lyapunov exponent we start at a random point at a point $\mathbf{x_0}$, at a distance $\delta_0 = 10^{-6}$ from the strange atractor and simulate for dimensionless time of 50. Then we add a second point $\mathbf{x_1}$ at a random position, s.t. $||\mathbf{x_1} - \mathbf{x_0}|| = 10^{-6}$. We integrate further over a time interval of 30 using both the initial conditions $\mathbf{x_0}$ and $\mathbf{x_1}$ and keep track of the separation distance $\delta(t)$. By performing a linear fit over the logarithm of the distance $\delta(t)$ the Lyapunov exponent λ is given by the slope of the line. Repeating this procedure with different initial conditions, gives slightly different values for λ. The true value of λ would be an average over a large number of iterations [2].

3. Results and Discussion

3.1. Poincaré Map and Cobweb Diagram

We start by calculating the Poincaré map of the trajectory of eq.(2.1.1).

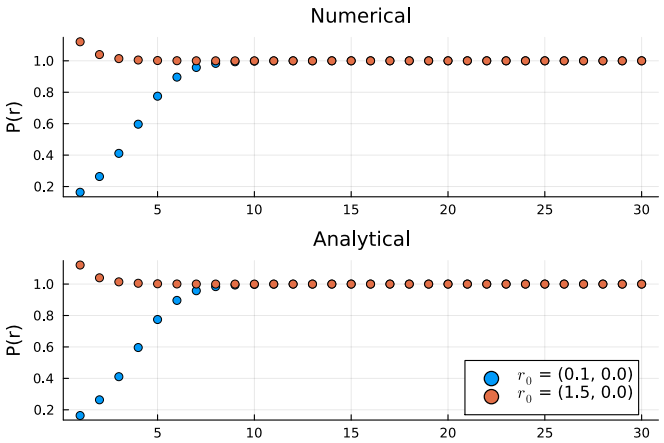

Figure 1: Comparison of numerical and analytical iterations of $P(r)$ over the first 30 steps. The top panel displays the numerical results, while the bottom panel presents the analytical computations. Both approaches start from initial conditions $r_0 = (0.1, 0)$ and $r_0 = (1.5, 0)$, shown in blue and orange respectively. The numerical integration is performed using a dimensionless timestep $\Delta t = 10^{-3}$.

We see qualitatively that the two figures are very similar, we can look into more detail and study the numerical error using eq. (2.1.4).

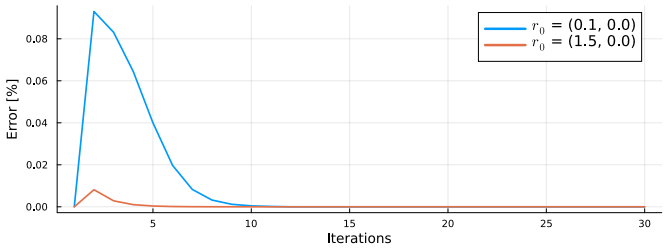

Figure 2: Relative error with different initial conditions r_0 over 30 iterations.

In figure 2 we see that the numerical method is fairly precise, with error no larger that 0.1% and it goes down very fast as the trajectory approaches the limit cycle at $r = 1$. With other words, we can find very good approximations

of where the fixed points on the Poincaré map are despite the numerical uncertainties.

It's obvious from fig. 1 that both plots converge towards $r = 1$. Hence, it seems natural to assume that there is a stable limit cycle there. To make sure we create a cobweb diagram, fig. 3 which confirms that intuition.

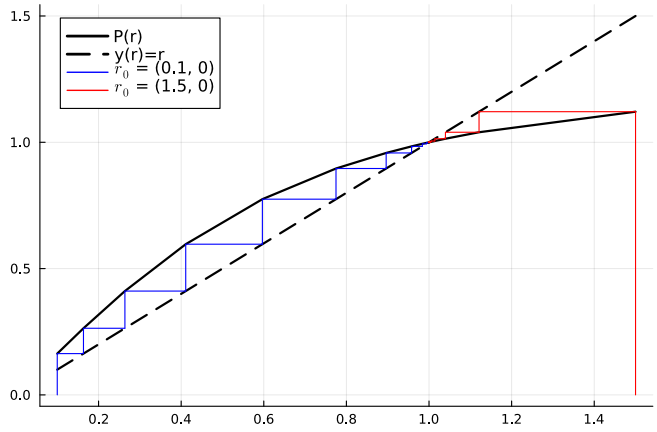

Figure 3: Cobweb diagram starting from two different initial conditions r_0. The dashed line represents the identity line $y = r$, the intersections with $P(r)$ denote fixed point. Both trajectories starting from $r_0 = (0.1, 0)$ and $r_0 = (1.5, 0)$ converge towards a fixed point at $r = 1$.

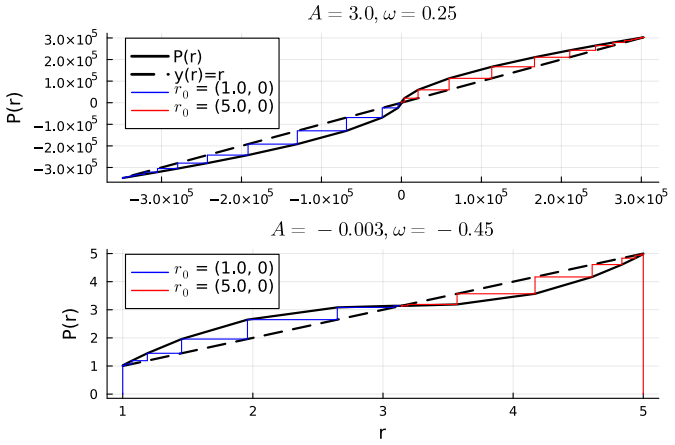

Figure 4: Two sets of Poincaré map iterations $P(r)$ for different parameter values of A and ω. The numerical integration is performed using a dimensionless timestep $\Delta t = 10^{-3}$. The upper panel corresponds to $A = 3.0, \omega = 0.25$, showcasing the trajectories from initial points $r_0 = (1.0, 0)$ and $r_0 = (5.0, 0)$ in black and red respectively. The lower panel represents $A = -0.003, \omega = -0.45$, with the blue and red curves illustrating the paths from the same respective starting points. Both panels display the function $y(r)$ as a dashed line, against which the iterative behavior of $P(r)$ is contrasted, revealing the dynamic stability or instability at various radii r.

Integrating numerically eq. (2.1.2) for different values of A and ω we obtain Poincaré map of the system that results in the Cobweb diagram given by fig. 4. We see that the Poincaré map has a fixed point at $r^* = 3$ representing a limit cycle of the system. For positive values of A the limit cycle is unstable and the trajectories diverge rapidly away from it. For values of $A < 0$ we see that both trajectories go towards r^* meaning that the system has a stable limit cycle at that point. ω can be chosen relatively freely as long as its value allows the two graphs to cross at a point.

3.2. Lorenz equations

We integrate numerically Lorenz equations (eq. 2.2.1) using adaptive Tsit5(4) method with adaptive stepsize for an interval of 50. The absolute and relative error tolerance is 10^{-9}. Using initial condition $x_0 = y_0 = z_0 = 0.001$. This results in the well known butterfly pattern.

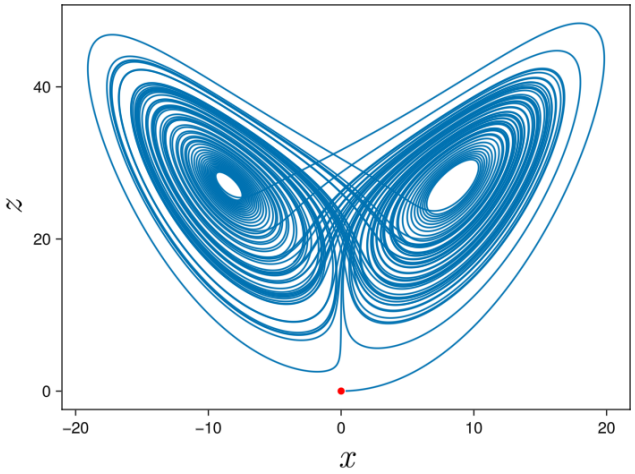

Figure 5: Trajectory of the Lorenz Attractor depicting chaotic dynamics in the xz - plane of a three-dimensional phase space. The red point denotes the initial position.

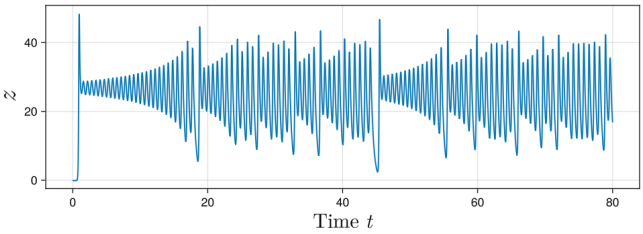

Figure 6: Time series plot of the z-variable in the Lorenz system, exhibiting irregular oscillations characteristic of chaotic behavior.

Now let's integrate over a longer time interval of 10^5. Let z_n be the peaks of z of the Lorenz system. The data from the chaotic time series appear to fall neatly on a curve with almost no "thickness" to the graph. Let us plot the identity line $y = z_n$ as well.

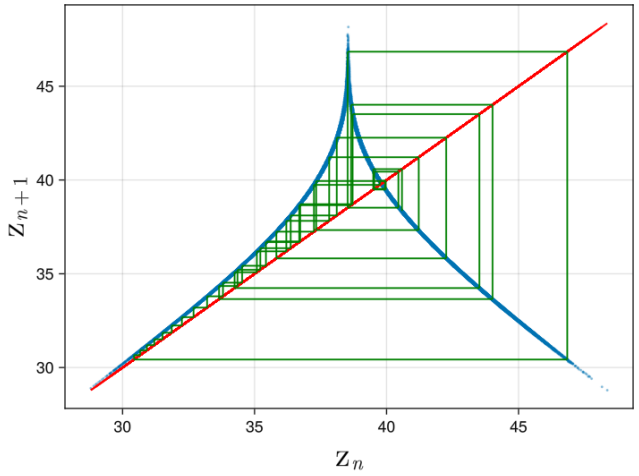

Figure 7: Cobweb diagram for the Lorenz system's peak values z_n. The peaks z_n are denoted in blue, the identity line in red. The figure shows the chaotic progression over iterations without convergence to a stable limit cycle, as evidenced by the divergent paths away from the line of identity $y = z_n$.

We see in the Cobweb diagram that even though the trajectories go arbitrary close to the intersection between the two curves, it never actually settles in a point showing that closed orbits are not possible in this system.

Let's define two random initial points $\mathbf{x}_0$ and $\mathbf{x}_1$ at a distance $||\mathbf{x_0} - \mathbf{x_1}||$ from each other.

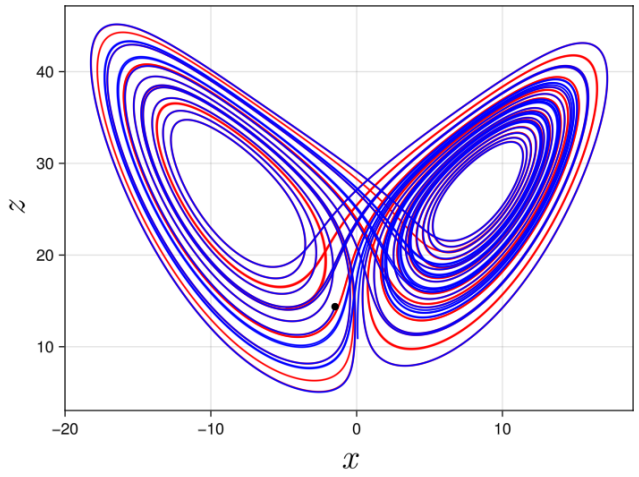

Figure 8: Trajectories in the Lorenz system for two slightly different initial conditions in the xz - plane of a three-dimensional phase space. The black point denotes the initial position.

We see that despite starting very close to each other they diverge quickly. This is to be expected as the separation distance between two points on the strange attractor should increase exponentially.

3.3. Rössler system

We integrate Rössler's equations using the same method and error tolerances as with the Lorenz system for a time interval of 300, initial condition $x_0 = y_0 = z_0 = 0.001$.

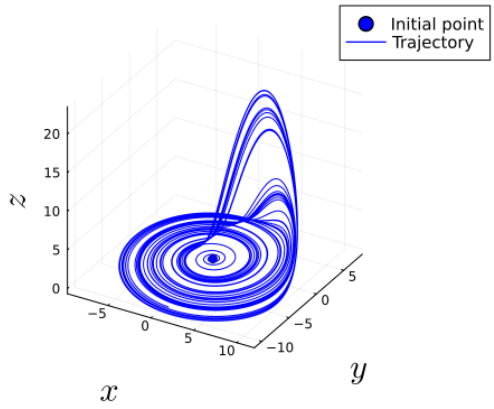

Figure 9: Three-dimensional plot of the Rössler system, showing the complex trajectory spiraling outwards from the initial point, characteristic of chaotic systems.

Once again integrating over an interval of 10^5 and plotting the peaks z_n of z of the Rössler system we find that they appear to follow a pattern.

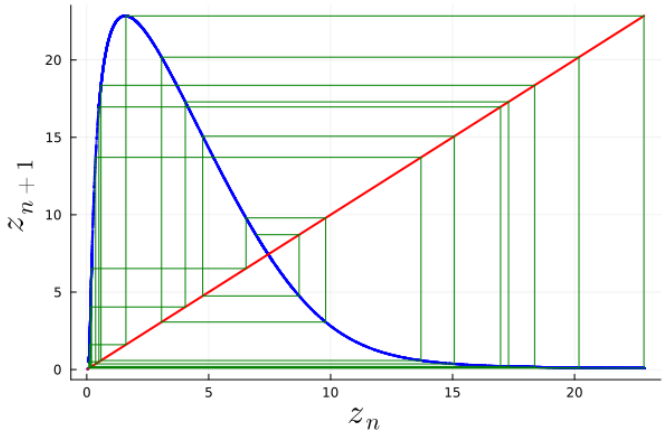

Figure 10: Cobweb diagram for the Rössler system's peak values z_n. The peaks z_n are denoted in blue, the identity line in red. Similarly to fig. 7 it illustrates a chaotic progression without convergence to a limit cycle, as shown by the divergent paths away from the line of identity $y = z_n$

3.4. Lyapunov exponents

As we have seen earlier two trajectories that start very close diverge quickly. More specifically the distance increases exponentially as given by eq. 2.2.3.

We start with the Lyapunov exponent of the Lorenz system.

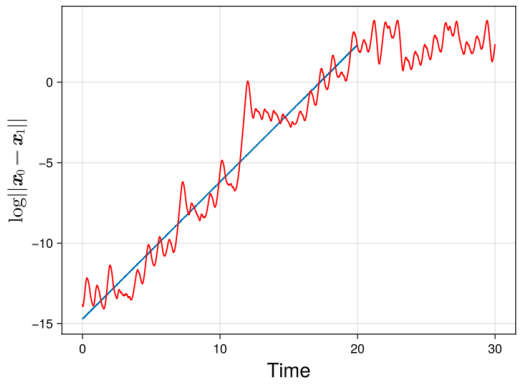

Figure 11: Logarithmic plot of the divergence of two nearby trajectories in the Lorenz system, demonstrating exponential separation over time.

As expected the separation distance grows exponentially until some cutoff time $T_c \approx 20$ where it flattens out. The divergence stops when the distance is comparable to the diameter of the attractor as the trajectories can't get any farther apart than that.

The situation is qualitatively similar in the case of the Rössler system.

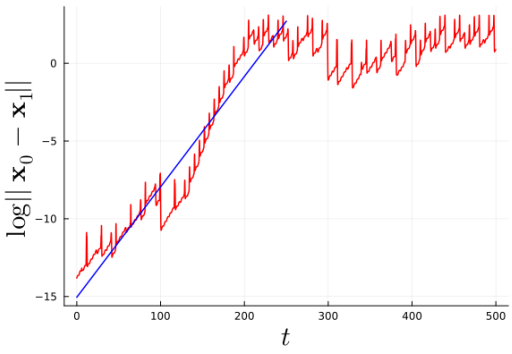

Figure 12: Logarithmic plot of the divergence of two nearby trajectories in the Rössler system, demonstrating exponential separation over time.

Fitting a line to the graph before the cutoff time and finding its slope we obtain slightly different values for the Lyapunov exponent. Repeating this procedure 100 times in the case of the Lorenz system, and 10 times for the Rössler system, and averaging the results gives us the values in table 1.

Table 1: The first Lyapunov exponents λ_{avg} for both the Lorenz and Rössler systems compared to the tabulated value of λ_{tab} as given in [4].

System	λ_{avg}	$\lambda_{tab} \pm 0.0005$
Lorenz ($\rho = 28$)	0.8672	0.9051
Rössler	0.0635	0.0696

We see that the values for the Lyapunov exponents of the two systems are very close to the tabulated values. A better estimation could be obtained by averaging over a larger number of trajectories but this is highly computationally demanding and is besides the purpose of this project.

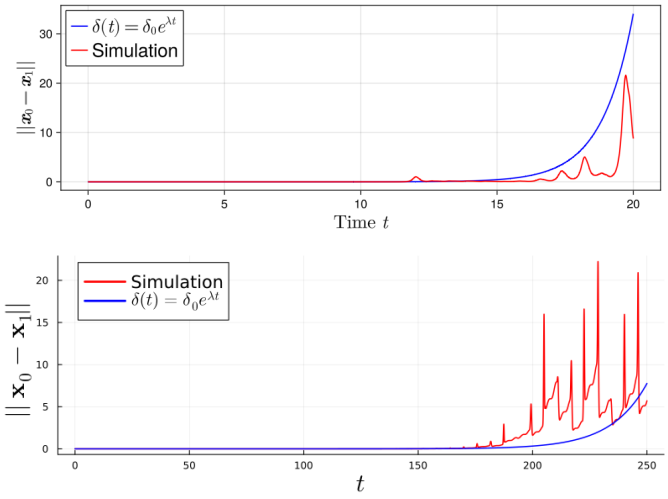

Figure 13: Comparative illustration of divergence in chaotic systems: the upper plot shows the Lorenz system's divergence from initial conditions, while the lower plot depicts the Rossler system's trajectory, both highlighting exponential separation over time. The λ in the expression in the legend corresponds to λ_{avg} for the respective system.

4. Conclusion

The investigation into the Poincaré maps and cobweb diagrams shows the power of those methods in analysing the stability of dynamical systems. Cobweb diagrams were then used to affirm the chaotic nature of the Lorenz and Rössler systems by showing there are no stable limit cycles within the studied parameter space. We computed the Lyapunov exponents that are in reasonable agreement with established values, confirming the robustness of our methods.A better estimation could be obtained by averaging over a larger sample size is needed. This study not only validates the chaotic nature of the Lorenz and Rössler systems but also displays the power of computational tools in analyzing complex dynamical systems.

References

[1] Strogatz, Steven. (2015). Nonlinear dynamics and chaos : with applications to physics, biology, chemistry, and engineering. Boulder, CO :Westview Press, a member of the Perseus Books Group.

[2] Dommersnes, Paul G. (2024). Numerical exercise TFY4305/FY8910 Nonlinear dynamics.

[3] Tsitouras, Charalampos. (2011). Runge–Kutta pairs of order 5(4) satisfying only the first column simplifying assumption. Computers & Mathematics with Applications. 62. 770-775. 10.1016/j.camwa.2011.06.002.

[4] Bovy, J., Bovy, J. (2004). Lyapunov Exponents and Strange Attractors in Discrete and Continuous Dynamical Systems.